

Magnetic fluctuations above the Néel temperature in κ -(BEDT-TTF)₂Cu[N(CN)₂]Cl, a quasi-2D Heisenberg antiferromagnet with Dzyaloshinskii–Moriya interaction

Ágnes Antal¹, Titusz Fehér¹, Bálint Náfrádi², László Forró², and András Jánossy^{*,1}

¹Budapest University of Technology and Economics, Institute of Physics and Condensed Matter Research Group of the Hungarian Academy of Sciences, P.O. Box 91, 1521 Budapest, Hungary

²Institute of Physics of Complex Matter, FBS, Swiss Federal Institute of Technology (EPFL), 1015 Lausanne, Switzerland

Received 14 October 2011, revised 2 November 2011, accepted 3 November 2011

Published online 16 March 2012

Keywords electron spin resonance, fluctuations, layered crystals, organic conductors, quasi-two-dimensional

* Corresponding author: e-mail atj@szfki.hu, Phone: +3614631391

We report on magnetic fluctuations studied by electron spin resonance (ESR) spectroscopy in the layered organic crystal κ -(BEDT-TTF)₂Cu[N(CN)₂]Cl. A line broadening above the antiferromagnetic ordering temperature, $T_N = 23$ K is attributed

to two-dimensional magnetic fluctuations of a staggered magnetization induced by the interplay of the magnetic field and the Dzyaloshinskii–Moriya (DM) interaction.

© 2012 WILEY-VCH Verlag GmbH & Co. KGaA, Weinheim

1 Introduction κ -(BEDT-TTF)₂Cu[N(CN)₂]Cl (hereafter κ -ET₂-Cl) is a strongly anisotropic layered organic crystal on the insulating side of a nearby metal–insulator Mott transition. Anionic polymer sheets in the (*a*, *c*) plane separate the organic ET layers. The electronic transport and magnetic properties are quasi two-dimensional. At high temperatures in the conducting bad metal phase the two dimensionality of the spin transport means that electrons remain confined to single molecular layers within the spin relaxation time [1]. The space group is P_{nma} [2, 3]; and the unit cell contains two chemically equivalent *a*–*c* layers, *A* and *B* in which the long axes of ET molecules are inclined from the *b* axis in opposite directions. At room temperature the crystal is a bad metal. Below 50 K it becomes insulating, while at $T_N = 23$ K a 3D ordered antiferromagnetic state develops [4].

In this paper we study magnetic fluctuations in κ -ET₂-Cl between T_N and 50 K by high sensitivity electron spin resonance (ESR) spectroscopy at several frequencies in magnetic fields up to 15 T. Spin fluctuations increase the ESR linewidth due to the increase of the transverse, $1/T_2$ or longitudinal spin relaxation rate, $1/T_1$. Between T_N and about 50 K the Dzyaloshinskii–Moriya (DM) interaction gives rise to magnetic field dependent ESR linewidth and shift.

Although the DM antisymmetric exchange interaction, $D \approx 3.7$ T [1] is small relative to the isotropic antiferromag-

netic exchange interaction of about $J = 450$ T [5, 6], it plays an important role in the magnetic properties. It is responsible for weak ferromagnetism in the antiferromagnetic ground state. The weak ferromagnetism appears spontaneously at the Néel temperature, $T_N = 23$ K [4], while above the Néel temperature the DM interaction gives rise to a magnetic field induced staggered magnetization [9]. The DM vector is in the (*a*, *b*) plane, inclined by 10° from the long axis of the ET molecules. D_A and D_B , the DM vectors of the *A* and *B* layers, respectively, are approximately perpendicular to each other. In magnetic fields, H , oriented along $\varphi_{ab} = 45^\circ$ in the (*a*, *b*) plane the ESR lines of the two layers are resolved and the linewidths are simultaneously measured in the *A* and *B* layers with $H \parallel c \times D_A$ and $H \parallel D_B$, respectively. In the temperature range of 25–50 K fields in the plane perpendicular to the DM vector induce strong in-plane polarized magnetic fluctuations, while fields parallel to the DM vector do not change the fluctuation spectrum. The interaction between adjacent layers is weak. Here, we show that the magnetic-field-induced fluctuations of adjacent layers are uncorrelated.

2 Experimental The κ -ET₂-Cl single crystals with typical dimensions of $1 \times 1 \times 0.2$ mm³ were grown by standard electrochemical oxidation of ET in Ar gas filled electrolytic cells. Crystal quality was verified by X-ray

diffraction. The high field ESR measurements were performed on home built quasi optical continuous wave spectrometers operating at 111.2 GHz and at 222.4 GHz at BME [7] and at 210, 315, and 420 GHz at EPFL [8]. For the low field measurements at 9.4 GHz at EPFL we used a Bruker ELEXSYS E500 spectrometer.

3 Results The interplay of the DM interaction and magnetic fields induces a staggered magnetization in the ET planes above the Néel temperature, T_N . A snapshot of the magnetic structure is shown in Fig. 1. The staggered magnetization is perpendicular to the DM vector and to the magnetic field and is largest for $\mathbf{H} \perp \mathbf{D}$. Interchanging the magnetic sublattices increases the energy and this leads to a non-zero temporal average, *i.e.*, to a static staggered magnetization (Fig. 1a). The static component is observed by an ESR line shift while fluctuations at the electronic Larmor frequency of this ordered moment broaden the ESR spectrum above T_N . For $\mathbf{H} \parallel \mathbf{D}$ spins rotate freely in the plane perpendicular to the magnetic field and there is no static staggered moment (Fig. 1b).

3.1 Temperature and field dependence of the ESR The ESR resonance position as a function of temperature at 420 GHz and $\mathbf{H} \parallel \mathbf{b}$ is shown in Fig. 2. The conduction electron resonance at high temperatures changes to an antiferromagnetic resonance on cooling below 23 K. There is a small temperature interval near T_N where the strong broadening renders the AFMR and the CESR unobservable. The transition from the paramagnetic to the antiferromagnetic state is accompanied by a large shift of the resonance position. Below 16 K the AFMR line splits into two lines. In the antiferromagnetically ordered state there are four resonance modes. For $\mathbf{H} \parallel \mathbf{b}$ the other two modes are shifted

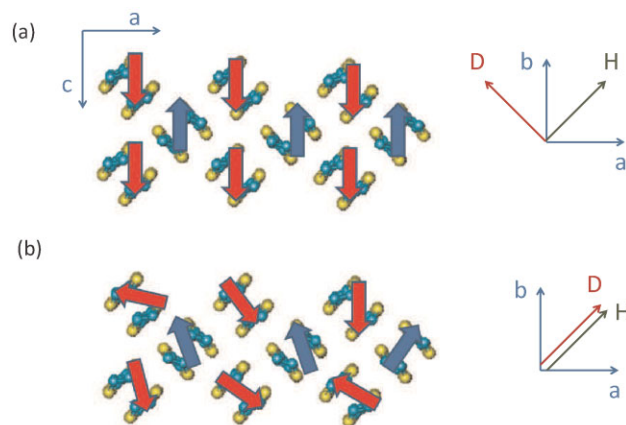


Figure 1 (online color at: www.pss-b.com) Snapshots of the magnetic structure slightly above T_N in the (a, c) plane, projected along the long ET molecular axis. (a) For $\mathbf{H} \perp \mathbf{D}$ the magnetic field induces a static staggered magnetization. The sublattice magnetic moments (blue and red arrows) are somewhat inclined from c . (b) For $\mathbf{H} \parallel \mathbf{D}$ the spins reorient freely in the plane perpendicular to \mathbf{H} and \mathbf{D} and there is no static staggered magnetization above T_N .

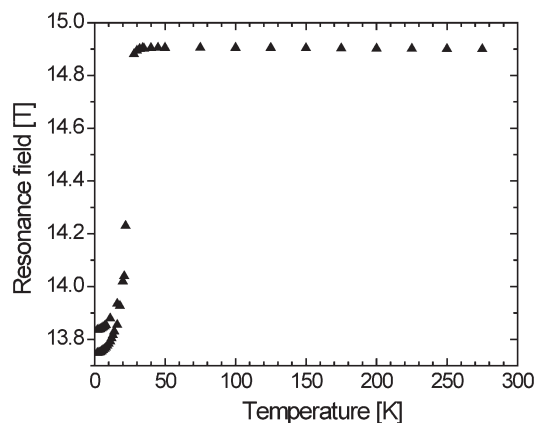


Figure 2 ESR resonance field at 420 GHz with $\mathbf{H} \parallel \mathbf{b}$. A strong shift accompanies the antiferromagnetic transition. Below 16 K two antiferromagnetic resonance modes are observable, two other modes are at higher fields.

to higher fields, they were observed at 111.2 GHz [1]. The AFMR lines continuously narrow in the 3D ordered state as the temperature is lowered (not shown). An analysis of the AFMR mode diagram shows that interlayer coupling between the A and B layers is extremely small [1].

In Fig. 3 a selection of data at 9.4, 111.2 and 222.4 GHz demonstrates the magnetic field strength and orientation dependence of the linewidths above T_N . The linewidths in the $\mathbf{H} \parallel \mathbf{c} \times \mathbf{D}_A$ and in the $\mathbf{H} \parallel \mathbf{D}_B$ directions were determined simultaneously from the resolved ESR lines of the A and B layers. In the $\mathbf{H} \parallel \mathbf{c} \times \mathbf{D}_A$ direction the field-induced increase of the linewidth below 50 K is much steeper at 222.4 GHz ($H \sim 8$ T) than at 111.2 GHz ($H \sim 4$ T) (Fig. 3). A similar field dependent line broadening was observed in the $\mathbf{H} \parallel \mathbf{c}$ direction (not shown). The linewidth at 9.4 GHz ($H \sim 0.3$ T) is small in all directions and is isotropic in the (a, b) plane. The linewidth is field independent for $\mathbf{H} \parallel \mathbf{D}_B$.

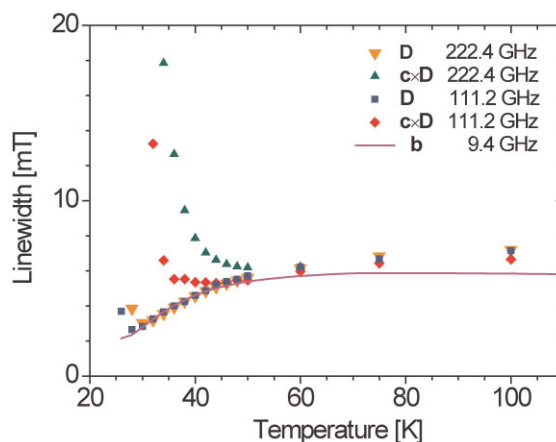


Figure 3 (online color at: www.pss-b.com) Magnetic field orientation and strength dependence of the linewidth. The line broadens below 50 K if $\mathbf{H} \perp \mathbf{D}$. The broadening increases with increasing magnetic field. There is no field induced broadening when $\mathbf{H} \parallel \mathbf{D}$.

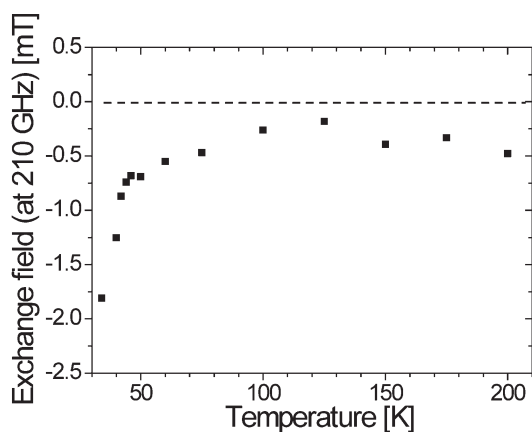


Figure 4 Temperature dependence of the exchange field between adjacent layers in κ -ET₂-Cl measured at 210 and at 315 GHz. The exchange field is proportional to the external field and is given for the measurement at 210 GHz. The dashed line is a guide to the eye at zero exchange field. An antiferromagnetic interaction between adjacent layers increases with decreasing temperature below 50 K.

3.2 Interlayer exchange interaction The exchange interaction between layers *A* and *B* is expressed as an effective magnetic field $\mathbf{H}_{\text{eff}AB} = \lambda \mathbf{M}_B$ where $\mathbf{H}_{\text{eff}AB}$ is the effective magnetic field in layer *A* due to the magnetization \mathbf{M}_B of layer *B* and λ is the coupling strength. The interlayer coupling changes the ESR lineshape, it is not simply a sum of the spectra of the adjacent layers. Figure 4 displays the temperature dependence of λ determined from the ESR spectrum in the $\varphi_{ab} = 45^\circ$ direction where the lines, parallel to \mathbf{D} and perpendicular to \mathbf{D} , are resolved [10]. The interaction between neighboring layers is antiferromagnetic and increases with decreasing temperature below 50 K.

4 Discussion Below 50 K there is a bad metal to insulator transition. The paramagnetic insulator state above T_N is not measurably affected by the small magnetic fields used in the 9.4 GHz experiments. At higher frequencies, however, the linewidth has a more complicated temperature dependence (Fig. 3). In the plane perpendicular to the DM vector the linewidth increases as T_N is approached. On the other hand, the ESR line narrows for $\mathbf{H} \parallel \mathbf{D}$. The broadening in $\mathbf{H} \perp \mathbf{D}$ direction increases with magnetic field. The interplay of the DM interaction and the external field induces a staggered magnetization perpendicular to the applied field and the DM vector as proposed by [9]. The fluctuations of the induced magnetization in the plane perpendicular to the DM vector at the ESR Larmor frequency increase the ESR linewidth. The narrowing of the ESR for $\mathbf{H} \parallel \mathbf{D}$ is independent of magnetic field and is not related to the DM interaction. In external magnetic fields oriented along $\varphi_{ab} = 45^\circ$ the fluctuating induced staggered magnetization broadens the line in the *A* layers while in the *B* layers there are no field induced fluctuations. The Néel temperature for the appearance of a spontaneous staggered magnetization is not increased by interlayer interactions.

4.1 Two-dimensional nature of field induced fluctuations

The simultaneous measurement of the *A* and *B* layer linewidths in the $\varphi_{ab} = 45^\circ$ orientation shows that the linewidth increase in *A* is not correlated to the increase in *B*. As a consequence of the extreme isolation between layers of κ -ET₂-Cl, fluctuations are independent in adjacent layers. For $\varphi_{ab} = 45^\circ$ the magnetic field is oriented $\mathbf{H} \parallel \mathbf{c} \times \mathbf{D}_A$ in layer *A* and $\mathbf{H} \parallel \mathbf{D}_B$ in layer *B*. (Here φ_{ab} denotes the angle from *a* in the (*a*, *b*) plane.) There is a strong line broadening in layers with $\mathbf{H} \parallel \mathbf{c} \times \mathbf{D}$ and no line broadening in layers with $\mathbf{H} \parallel \mathbf{D}$ orientation (Fig. 3). The linewidth in the *c* direction (not shown), where $\mathbf{H} \perp \mathbf{D}$ in both layers the linewidth broadens similarly as for $\mathbf{H} \parallel \mathbf{c} \times \mathbf{D}_A$. We conclude that fluctuations in one layer do not affect fluctuations in the adjacent layer. Thus, there is no measurable three-dimensional correlation in the fluctuations.

4.2 Inter-layer exchange interaction There is a small static exchange interaction between adjacent layers. The coupling constant λ between *A* and *B* layers derived from the detailed line shape analyses of $\varphi_{ab} = 45^\circ$ spectra [10] is shown in Fig. 4. The antiferromagnetic interaction between adjacent layers increases with decreasing temperature below 50 K, in the same temperature range where the staggered magnetization develops. The temperature dependence of λ in κ -ET₂-Cl above the Néel temperature is similar to λ measured in the conductor, κ -ET₂-Br in the same temperature range [10].

4.3 Assignment of ESR lines Smith et al. [5] showed that due to symmetry reasons the DM vector must be perpendicular to *c*. According to previous NMR and ESR measurements [5, 1] the DM vectors lie in the (*a*, *b*) plane in the directions $\varphi_{ab} = 46^\circ$ and 134° , so the DM vector of two neighboring layers are nearly perpendicular to each other. A further consideration is required to decide which DM direction corresponds to which layer. Nakamura et al. [11] measured the ESR *g*-factor anisotropy of several ET salts. They found that in κ -ET₂-X salts the maximal *g*-factor is along the long molecular axis. This allows the assignment of the ESR lines to the corresponding *A* and *B* layers. The DM vector is inclined 10° (and not 100°) from the long axis of the ET molecules if one assumes that the ESR line is broadened most in external fields perpendicular to the DM vector.

5 Conclusions Magnetic fluctuations due to the DM interaction in κ -ET₂-Cl layered crystals were studied by ESR. These fluctuations lie in the plane perpendicular to the DM vector and increase with increasing magnetic field. The fluctuations in adjacent layers are independent. We observed a small static antiferromagnetic exchange between neighboring layers, λ that is assumed to be proportional to the external field. λ increases with decreasing temperature below the bad-metal to insulator transition.

Acknowledgements The authors thank N. D. Kushch (Inst. of Problems of Chemical Physics, Chernogolovka, Russia) for

instructions on crystal growth. The work is supported by the ERC Grant Nr. ERC-259374-Sylo. We acknowledge the support of the Hungarian National Research Fund OTKA NN76727, CNK80991, the New Hungary Development Plan TÁMOP-4.2.1/B-09/1/KMR-2010-0002, and the Swiss NSF and its NCCR “MaNEP”. T. F. acknowledges support from the János Bolyai program of the Hungarian Academy of Sciences.

References

- [1] Á. Antal, T. Fehér, A. Jánossy, E. Tátrai-Szekeres, and F. Fülöp, *Phys. Rev. Lett.* **102**, 086404 (2009).
- [2] J. M. Williams, A. M. Kini, H. H. Wang, K. D. Carlson, U. Geiser, L. K. Montgomery, G. J. Pyrka, D. M. Watkins, J. M. Kommers, S. J. Boryschuk, A. V. S. Crouch, W. K. Kwok, J. E. Schirber, D. L. Overmyer, D. Jung, and M. H. Whangbo, *Inorg. Chem.* **29**, 3272–3274 (1990).
- [3] A. M. Kini, U. Geiser, H. H. Wang, K. D. Carlson, J. M. Williams, W. K. Kwok, K. G. Vandervoort, J. E. Thompson, D. L. Stupka, D. Jung, and M. H. Whangbo, *Inorg. Chem.* **29**, 2555–2557 (1990).
- [4] U. Welp, S. Fleshler, W. K. Kwok, G. W. Crabtree, K. D. Carlson, H. H. Wang, U. Geiser, J. M. Williams, and V. M. Hitsman, *Physica B* **188**, 1065–1067 (1993).
- [5] D. F. Smith, S. M. De Soto, C. P. Slichter, J. A. Schlueter, A. M. Kini, and R. G. Daugherty, *Phys. Rev. B* **68**, 024512 (2003).
- [6] D. F. Smith, C. P. Slichter, J. A. Schlueter, A. M. Kini, and R. G. Daugherty, *Phys. Rev. Lett.* **93**, 167002 (2004).
- [7] K. L. Nagy, D. Quintavalle, T. Feher, and A. Jánossy, *Appl. Magn. Reson.* **40**, 47–63 (2011).
- [8] B. Nafradi, R. Gaal, T. Feher, and L. Forró, *J. Magn. Reson.* **192**, 265–268 (2008).
- [9] F. Kagawa, Y. Kurosaki, K. Miyagawa, and K. Kanoda, *Phys. Rev. B* **78**, 184402 (2008).
- [10] Á. Antal, T. Fehér, E. Tátrai-Szekeres, F. Fülöp, B. Náfrádi, L. Forró, and A. Jánossy, *Phys. Rev. B* **84**, 075124 (2011).
- [11] T. Nakamura, T. Nobutoki, T. Takahashi, G. Saito, H. Mori, and T. Mori, *J. Phys. Soc. Jpn.* **63**, 4110–4125 (1994).